World Applied Sciences Journal 13 (4): 781-790, 2011
ISSN 1818-4952
© IDOSI Publications, 2011

Investigation of Temperature and Influent Load on Nitrifying Treatment of Using Wastewater CFD

Baharak Sajjadi, Mostafa Keshavarz Moraveji and Reza Davarnejad

Department of Chemical Engineering, Faculty of Engineering,
Arak University, Arak 38156-8-8349, Iran

Abstract: The paper describes the effect of temperature, ammonia concentration and feed flow rate on nitrifying treatment of wastewater usage Computational Fluid Dynamics (CFD) for two phase bubbly flow in a split cylindrical airlift reactor with a 0.085 m initiator diameter and 0.505 m height. Superficial gas velocity was used as the operational parameter, air was used as the dispersed phase and wastewater containing ammonia was used as continuous phase. Temperature enhancement in a constant O_2 and NH_4^+ concentrations, resulted the increase of reactions rate also NO_2^- had an increase of about 3 times as much. By the feed flow rate increase, O_2 consumption increase and the rate of NO_2^- production increase more than NO_3^- but decrease the reactions efficiency decrease in a constant time. NH_4^+ concentration enhancement leads to the increase of O_2 consumption and better reactions efficiency at higher NH_4^+ concentration, NO_2^- concentration increases more. Modeling results are compared with the experimental data. The CFD modeling results show suitable agreement with the experimental data.

Key words: Airlift reactor · Wastewater treatment · Nitrification · Free ammonia

INTRODUCTION

The world that we all live in and its development of technology and the industries, has created some problems in spite of making our lives more comfortable such as pollutions in soil, in water even in the air. Ammonia, nitrite and nitrate are some of the most harmful and common water pollutants which exist in many wastewaters. By injecting such wastewater to the environment running water and in continue to the cities piped water system, such material will be imported to human body. Gastric bacteria change the nitrite to nitrate and so influence on the digestion system, especially in children, in addition nitrite in stomach react with the amines, amides and produce nitroamine which will result gastric cancer after a long time [1-3].

In the environment running water ammonia ions are combined with oxygen and produce toxic materials, so oxygen concentration decreases and toxic material, increase which intimidate the aquatic life [4].

There are different methods for ammonia removal from wastewater, including physical-chemical processes, using filters, resins or osmosis methods and biological processes, but biological processes have a better efficiency and in a large scale, are more efficient economically so are investigated in many studies [2, 5]. Conventional biological nitrogen removal has two steps (nitrification and dinitrification) that carry out subsequently or simultaneously, but this process is just useful for a low ammonia concentration and needs two separate reactors, but lately new processes have been studied and used, such as ANAMMOX, SHARON, CANON, OLAND and so on, that are more efficient and just need one reactor, because they contain one slight nitrification step to nitrite and nitrite turens to nitrogen gas; so the nitrite change to nitrate doesn't happen and the amount of oxygen consumption decreases and they are useful in wastewater with high amount of ammonia or combined with nitrogen [6-10].

In these processes, setting the optimum conditions are so important to decrease costs and time, but to increase efficiency. Simulation is one of the best methods for finding optimum parameters.

Corresponding Author: Mostafa Keshavarz Moraveji, Department of Chemical Engineering, Faculty of Engineering, Arak University, Arak 38156-8-8349, Iran.
Tel: +98-9363098063, Fax: +98-861-4173450, E-mail: m-moraveji@araku.ac.ir.

Airlift bioreactors are one of the best equipments for two or three phase contacting. These reactors are characterized by many advantages such as suitable mixing without any movable section, closer contact between the phases, faster oxygen transfer rate, shorter reaction time and greater process capability. Changing and controlling the parameters are so easy in such reactors so they are suitable for biological processing like ammonia removal [11-12]. Several researchers have studied the hydrodynamics and mass transfer of nitrifying in bioreactors.

The influences of the bed (settled) volume on bioreactor volume ratio in a three-phase flow multiple airlift loop bioreactor, superficial air velocity Ug, hydraulic residence time HRT and pH value on ammonia nitrogen reduction were investigated by Jianping *et al.* [1].

Kouakoua *et al.* has developed a novel circulating a jet-loop submerged membrane bioreactor (JLMBR) adapted to ammonium partial oxidation [13]. This study is intended to determine how gas–liquid mass transfer is affected by operating conditions, in order to obtain a high biomass retention time and to achieve a separate control of mixing and aeration they have adopted membrane technology is adopted and air and water forced circulation are combined.

The effects of temperature and free ammonia of landfill leachate on nitrification and nitrite accumulation were investigated by Kim *et al.* [14] with a semi-pilot scale biofilm airlift reactor they have found High free ammonia inhibited both from nitrite oxidizing bacteria (NOB) and also ammonia oxidizing bacteria (AOB).

Kim *et al.* have developed a sequencing batch airlift reactor (SBAR) to selectively enrich ammonia oxidizers as the dominant nitrifying bacteria and granulate ammonia oxidizers from wastewater nitrification [15]. Partial nitrification and reduced settling time were the selection pressures for the selective enrichment and granulation of ammonia oxidizers. They also achieved stable partial nitrification to accumulate nitrite.

Mosquera-Corral *et al.* have studied effects of acetate and different salts present in feed of a SHARON reactor on partial nitrification of ammonia to nitrite the results indicate that the decrease in ammonia oxidizing activity was due to a competition for substrates between both heterotrophs and autotrophs bacteria [3].

Kempen *et al.* have constructed a SHARON system; they have found that due to the high ammonium influent concentrations pH control is of great importance and during a stable process, they removed 90% of N-ions via the nitrite route [16].

Astrid *et al.* have investigated, an autotrophic, synthetic medium for the enrichment of anaerobic ammonium-oxidizing (Anammox) microorganisms and they have shown acetylene, phosphate and oxygen to be strong inhibitors of Anammox activity [17].

Astrid *et al.* in another work have examined the Anammox process in detail. they have explained that the rate of ammonium oxidation was proportional to the initial amount of oxidizing sludge, also in addition chloramphenicol, ampicillin, 2,4-dinitroohenol, carbonyl cyanide *m*-chlorophenyl hydrazone and mercuric chloride completely inhibited the activity of the ammonium oidizing sludge [18].

Jetten *et al.* have suggested the combination of two processes (anammox and Sharon) [19] and Dijkmen, *et al.* have suggested the Cannon process using nitrite as an autotrophic for the first time and has had successful results [20].

The aim of the present study was to investigate the turbulence temperature, ammonia concentration and feed flow rate on nitrifying treatment of wastewater. CFD software was applied for this investigation.

Problem Definition

Conventional Nitrification and Denitrification: Conventional microbial nitrogen removal is based on autotrophic nitrification and heterotrophic denitrification. Conversion of NH_4^+ to NO_2^- and further to NO_3^-, with oxygen molecules as the electron acceptor, is called nitrification. The relevant reactions are as follow:

$$NH_4^+ + 1.5O_2 \rightarrow NO_2^- + 2H^+ + 2H_2O \quad (1)$$

$$NO_2^- + 0.5O_2 \rightarrow NO_3^- \quad (2)$$

The anoxic denitrification (conversion of NO_3^- and NO_2^- to nitrogen gaseous) is accomplished with a variety of electron donors, including methanol, acetate, ethanol, lactate and glucose. The anoxic denitrification involves the following reactions [21]:

$$2NO_3^- + 10H^+ + 10e^- \rightarrow N_2 + 2OH^- + 4H2O \quad (3)$$

$$2NO_2^- + 6H^+ + 6e^- \rightarrow N_2 + 2OH^- + 2H2O \quad (4)$$

In this writing, just the nitrification section has been simulated.

Modeling Equation: The classical Euler–Euler two fluid model was employed to simulate the bubbly flow for every phase.

The equation of continuity for each phase is

$$\frac{\partial(\varepsilon_k \rho_k)}{\partial t} + \nabla.(\varepsilon_k \rho_k u_k) = S_k \tag{5}$$

Where ε, ρ and u are gas hold-up, density and velocity in each phase, respectively. S_k represents a source term of phase k in the domain.

Momentum Equation Is Derived as Following:

$$\frac{\partial(\alpha_k \rho_k u_k)}{\partial t} + \nabla(\alpha_k \rho_k u_k . u_k) = -\alpha_k \nabla p + \alpha_k \rho_k g + \nabla.\alpha_k \tau_k \pm F_{\text{int}} \tag{6}$$

The right side of the above equation respectively shows pressure difference, gravity force, stress and the ensemble averaged momentum exchange between the intra-phase forces. The pressure is shared between the phases [22, 23].

The drag and lift forces can be determined using equations (5) and (6), respectively.

$$F_d = \frac{3}{4}\frac{C_D}{d_b}\rho_l \alpha_g \alpha_l \left|u_g - u_l\right|(u_g - u_l) \tag{7}$$

$$C_D = 0.622/(1/Eo + 0.235) \tag{8}$$

Where, d_b is bubble diameter, CD is the drag coefficient and Eo is Eotvos number [22].

$$F_l = -C_l \alpha_g \rho_l (u_g - u_l) \tag{9}$$

$$C_l = -0.06 \tag{10}$$

Where, CL is the lift coefficient.

The turbulent stresses can be evaluated using the following expression:

$$\tau_k = -\mu_{eff,k}\left(\nabla u_k + (\nabla u_k)^T - \frac{2}{3}I(\nabla.u_k)\right) \tag{11}$$

Where, μ_{eff} is the effective viscosity.

Turbulence Equations: The turbulent viscosity is governed by the $k - \varepsilon$ model [22] as following:

$$\mu_T = \rho_l C_\mu \frac{k^2}{\varepsilon} \tag{12}$$

The transport equation for the turbulent kinetic energy (k) and the evolution of the turbulent energy dissipation rate (ε) are defined as following:

$$\rho_l \frac{\partial k}{\partial t} - \nabla.\left[\left(\mu + \frac{\mu_T}{\sigma_k}\right)\nabla k\right] + \rho_l u_l.\nabla k = \frac{1}{2}\mu_T(\nabla u_l + (\nabla u_l)^T)^2 - \rho_l \varepsilon + S_k \tag{13}$$

$$\rho_l \frac{\partial \varepsilon}{\partial t} - \nabla.\left[\left(\mu + \frac{\mu_T}{\sigma_k}\right)\nabla \varepsilon\right] + \rho_l u_l.\nabla \varepsilon = \frac{1}{2}C_{\varepsilon 1}\frac{\varepsilon}{k}\mu_T(\nabla u_l + (\nabla u_l)^T)^2 - \rho_l C_{\varepsilon 2}\frac{\varepsilon^2}{k} + \frac{\varepsilon}{k}C_\varepsilon S_k \tag{14}$$

The model contains five parameters and those values were obtained from the literature as following [22, 24].

$C_\mu = 0.09$; $C_1 = 1.44$; $C_2 = 1.92$; $\sigma_k = 1.0$; $\sigma_\varepsilon = 1.3$

Convection and diffusion have been studied using the following expression:

$$\delta_{ts}\frac{\partial c\_C_n}{\partial t} + \nabla.(-D\nabla c\_C_n) = R - u.\nabla c\_NH_4 \tag{15}$$

Which C_n (n=1-4) are the concentration of (NH_4^+, NO_2-, NO_3^-, O_2) respectively.

In this simulation, there are two reactions that happen continuously because of the enthalpy and entropy and diffusion coefficient for its material both reactions are sensitive to temperature so the heat effects are considerable.

The combination of mass balance for (NH_4^+, NO_2^-, NO_3^- *and* O_2) constitutes a set of four second-order differential equations with the following expression:

$$\frac{1}{r^2}\frac{d}{dr}\left(r^2 De_n \frac{dC_n}{d_r}\right) + r_n = 0$$

Where rn is the net reaction rate and Den the diffusion coefficient of each compound. By solving the equation, reaction rates were obtained as follows in Table 1.

Table 1: Species settings [25]

Spices	Diffusivity	Init value	Rate expression
NH_4	D_NH_4	$C\_NH_4(t_0)$	$r_{NH4} = -\frac{\mu_{MAXAO}}{Y_{NAO}} \frac{C_{NH4}}{K_{SAO} + C_{NH4} + C_{NH4}^2 / K_{IAO}} \frac{C_{O2}}{K_{OAO} + C_{O2}} X_{AO}$
NO_2^-	D_NO_2	$0(t_0)$	$r_{NO2} = \frac{\mu_{MAXAO}}{Y_{NAO}} \frac{C_{NH4}}{K_{SAO} + C_{NH4} + C_{NH4}^2 / K_{IAO}} \frac{C_{O2}}{K_{OAO} + C_{O2}} X_{AO} - \frac{\mu_{MAXNO}}{Y_{NNO}} \frac{C_{NO2}}{K_{SNO} + C_{NO2} + C_{NO2}^2 / K_{INO}} \frac{C_{O2}}{K_{ONO} + C_{O2}} X_{NO}$
NO_3^-	D_NO_3	$0(t_0)$	$r_{NO3} = \frac{\mu_{MAXNO}}{Y_{NNO}} \frac{C_{NO2}}{K_{SNO} + C_{NO2} + C_{NO2}^2 / K_{INO}} \frac{C_{O2}}{K_{ONO} + C_{O2}} X_{NO}$
O_2	D_O_2	$C_0\_O_2(t_0)$	$r_{O2} = -\frac{\mu_{MAXAO}}{Y_{OAO}} \frac{C_{NH4}}{K_{SAO} + C_{NH4} + C_{NH4}^2 / K_{IAO}} \frac{C_{O2}}{K_{OAO} + C_{O2}} X_{AO} - \frac{\mu_{MAXNO}}{Y_{ONO}} \frac{C_{NO2}}{K_{SNO} + C_{NO2} + C_{NO2}^2 / K_{INO}} \frac{C_{NO2}}{K_{ONO} + C_{O2}} X_{NO}$

Table 2: Reaction setting

Reactions	Type	K_f	Kr	ΔG^0[$kjmol^{-1}$][3]	Reaction rate
NH4+2O2<=>NO2+2H2O	Reversible	1	0.2	-275	$K_f.C_{NH_4}.(C_{O_2})^2$
2NO2+O2=>2NO3	Irreversible	1	0	-295	$K_f.C_{O_2}.(C_{NO_2})^2$

Table 3: Heat setting

Reactions	Enthalpy of reaction	Entropy of reaction
NH4+2O2<=>NO2+2H2O	$-h_{NH_4} - 2.h_{O_2} + h.NO_2 + 2.h_{H_2O}$	$-s_{NH_4} - 2.s_{O_2} + s.NO_2 + 2.s_{H_2O}$
2NO2+O2=>2NO3	$-h_{O_2} - 2.h_{NO_2} + 2.h.NO_3$	$-s_{O_2} - 2.s_{NO_2} + 2.s.NO_3$

Table 4: Expression used [25]

Parameter	Expression
μ_{MAXAO}	$\exp(0.0951T - 2.174)$
μ_{MAXNO}	$\exp(0.058T - 1.13)$
K_{SAO}	$\exp(0.1174T - 2.666)$
K_{SNO}	$\exp(0.145T - 2.646)$
De_4	$fd_4 Dw_4 e^{(E/RT)}$
De_n	$fd_n Dw_n \frac{\eta_{25}}{\eta_T} \frac{T}{298.15}$

Reactions details and heat settings have been introduced in Tables 2, 3.

The reactor consists of a tubular section of 0.085 m interior diameter and 0.8 m height with a conic bottom used as a settler. The fluidization zone between the air injection and the liquid level is 0.505m high [25]. Half of the reactor has been selected for simulation and the processes were simulated at room temperature (25°C), except the simulation that concerns the temperature effects. For temperature effect simulation 15, 20, 25, 30°C were selected.

Feeding flow rate was 0.2, 0.6, 0.8 L/h which is water plus ammonia with the concentration of 250, 500, 750 mg/L. we assumed that 21% of air injection is oxygen and the rest is nitrogen and all of the oxygen is dissolved in the liquid. The bubbly flow regime was selected with the bubble size of $2_{\times}10^{-3}$ m [26-27].

RESULTS AND DISCUSSION

In Figure 1, boundary setting (Figure 1-a), mesh element sizes (Figure 1-b), liquid and gas streamlines (Figure 1-c), liquid and gas volume fraction (Figure 1-d, f) and materials concentrations have been shown consecutively at the aeration of 2.26 L/h. It can be seen that the gas leaves the reactor but the liquid circulates in it.

Because of air injection from the center and bottom of reactor, these bubbles containing O_2 are new and fresh in lower zone concentration also the volume fraction of air is higher in this zone, so most of the reactions carried out here result in NO_2^- concentration becoming more than the other places also both reactions were carried out continuously thus when the first molecules of NO_2^- produced the other, the reaction was carried out quickly and NO_3^- starts being produced and because the most of oxygen and NO_2^- is in here, the second reaction carried out here is more than any other place so there is more NO_3^- concentration here.

Effect of Temperature: Figure 2 shows the temperature effect. By starting the first reaction, NH_4^+ and O_2 decrease but the O_2 curve slope is more because it is consumed in two reactions.

About NO_2^-, at first, the production rate is more than NO_3^- because the amount of NH_4^+ that producces NO_2^- is more than NO_2^- that produces NO_3^- (at 25°C) until NH_4^+ is finished, at this point, NO_2^- production rate turns negative because it is consumed in the second reaction. In addition, about NO_3^- the curve has two slopes, when NO_2^- is produced, the NO_3^- production slope is more but when NH_4^+ is finished, with the slope of the NO_2^- production, NO_3^- producing slope decrease too. At high temperature the curve slope of NH_4^+ and O_2 consumption are more, because the reactions are carried out quickly so the NO_2^- production rate increases but at lower temperatures at first the NO_2^- curve is near the zero because NO_2^- production is little and as soon as a little NO_2^- is produced, it is consumed too. About NO_3^-, the curve has two slopes, at first where NO_2^- is produces, production rate of NO_3^- is high too, but as soon as the NO_2^- production finishes,

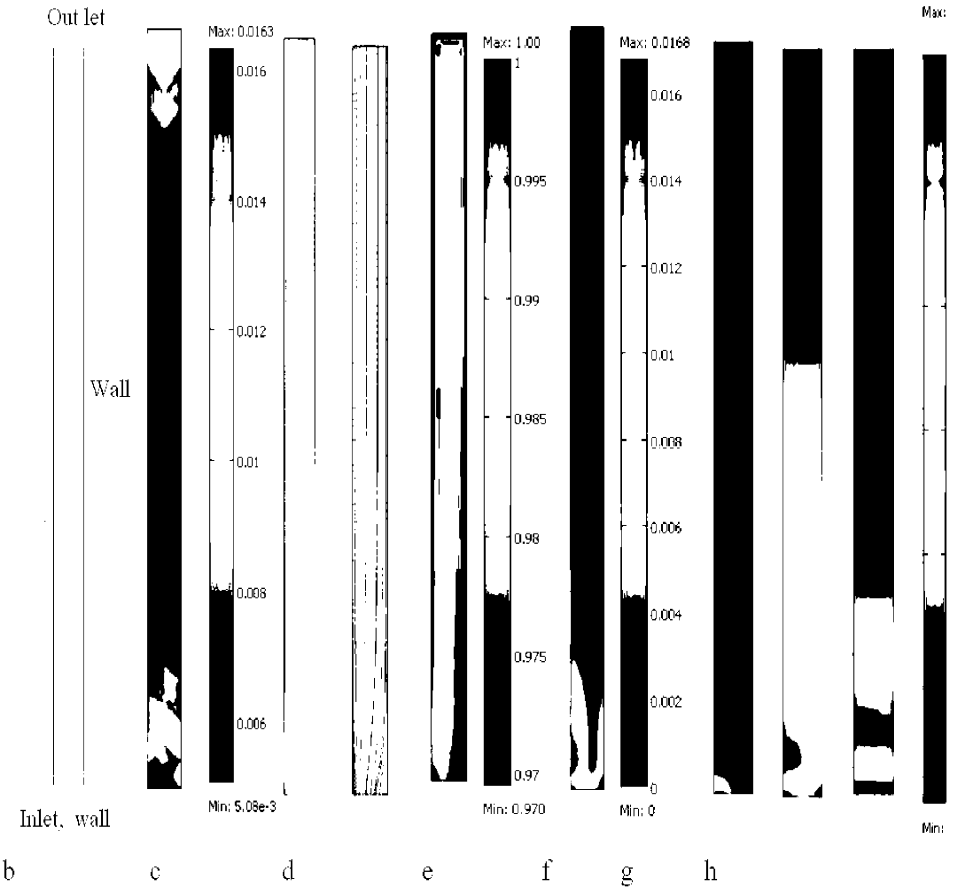

Fig. 1a: Boundary conditions, b:mesh details, c: liquid and gas stream lines, d: liquid volume fraction. e: gas volume fraction, f: O_2 concentration, g: NO_2^- concentration, h: NO_3^- concentration

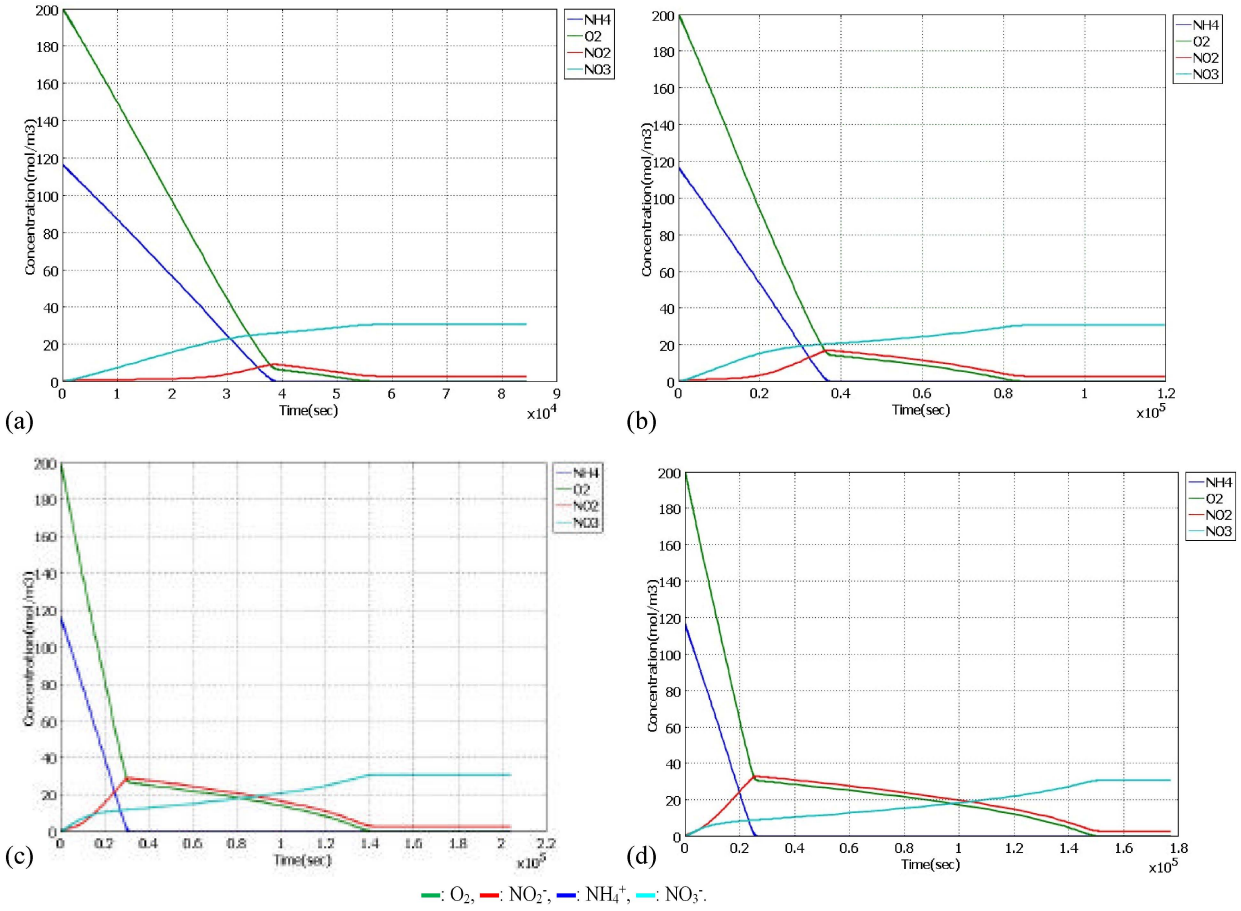

Fig. 2: Temperature effect. a) 15°C b)20°C c)25°C d)30°C at feed flow rate of 0.8 L/h with 250 mg/L NH_4^+

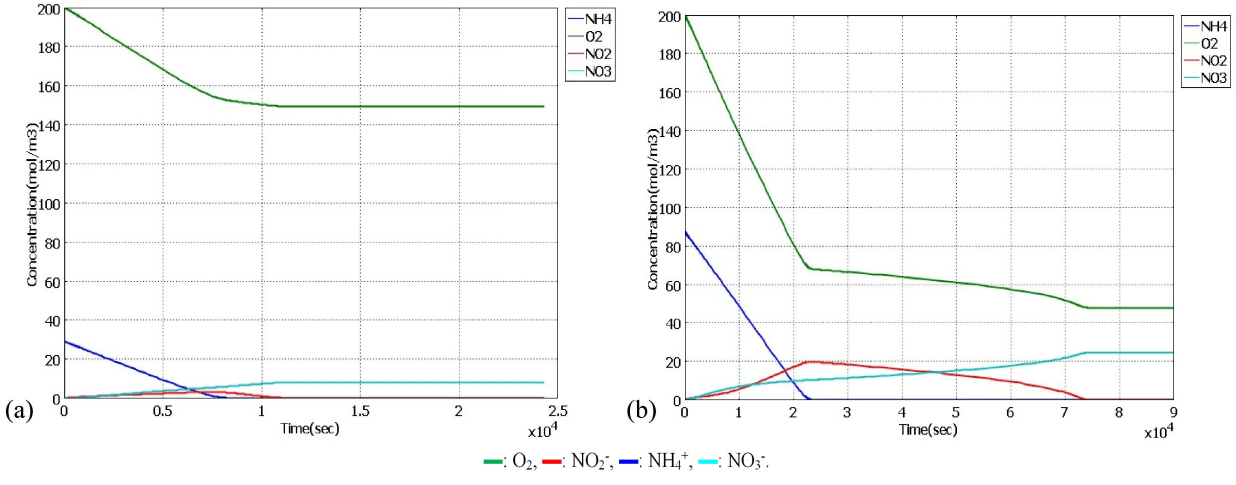

Fig. 3a: feed flow rate of 0.2L/h with 250 mg/L NH_4^+. b: at feed flow rate of 0.6 L/h with 250 mg/L NH_4^+ at 25°C

the rate of NO_3^- production decreases too. Generally, NO_3^- production rate depends on NO_2^-, meaning by increasing NO_2^- production, NO_3^- increase too and the opposite.

Effect of Feed Flow Rate: Figure 3, shows the effect of feed flow rate. Three different feed flow rates have been used 0.2, 0.6 and 0.8 L/h so that the last one is in Figure (2-c) at higher flow rate (0.6 L/h) the oxygen curve

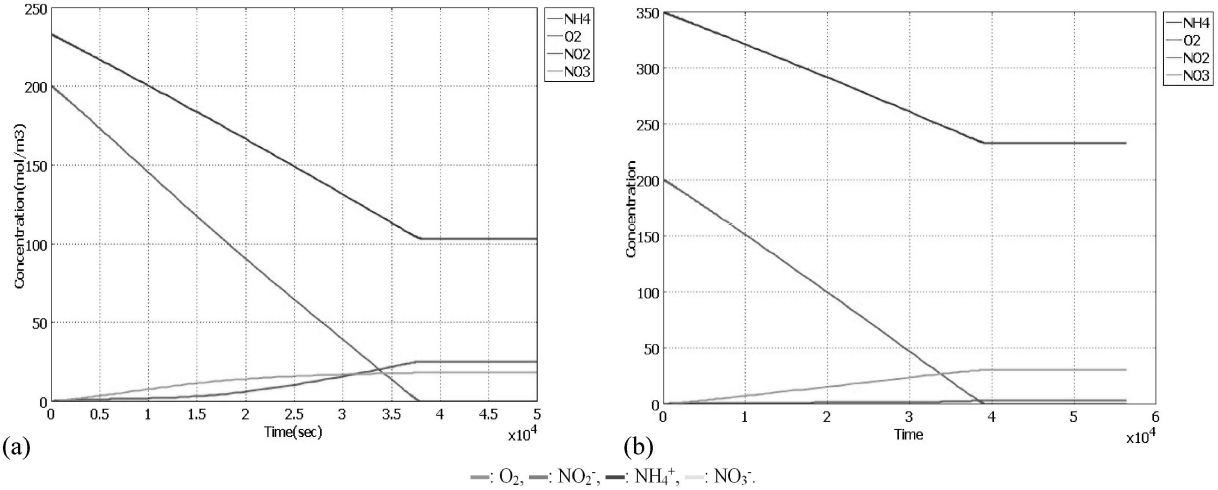

Fig. 4a: feed flow rate of 0.8L/h with 500 mg /L NH4 at 25°C. b: at feed flow rate of 0.8 L/h with 750 mg/L NH_4^+

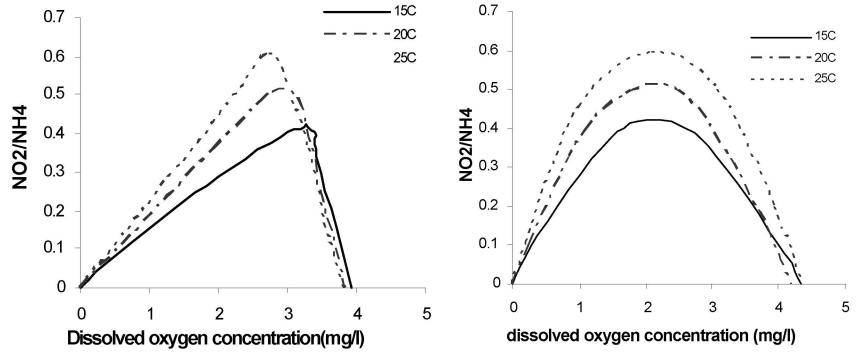

Fig. 5a: Temperature effect. Feeding flow rate of 0.8 L/h and 250 mg/L NH_4^+

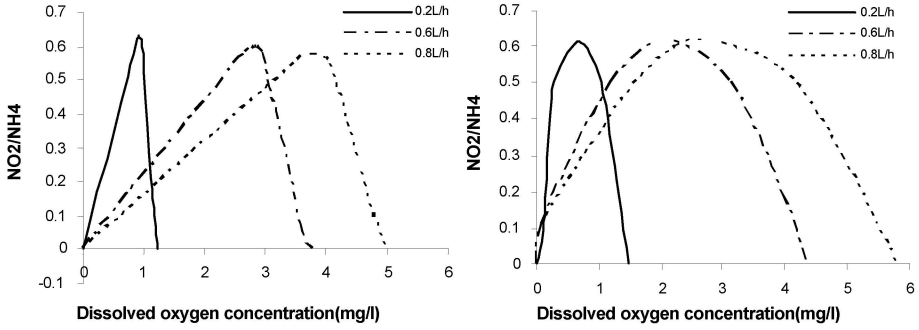

Fig. 5b: Feeding flow rate effect. 250 mg/L NH_4^+ concentration at 25°C

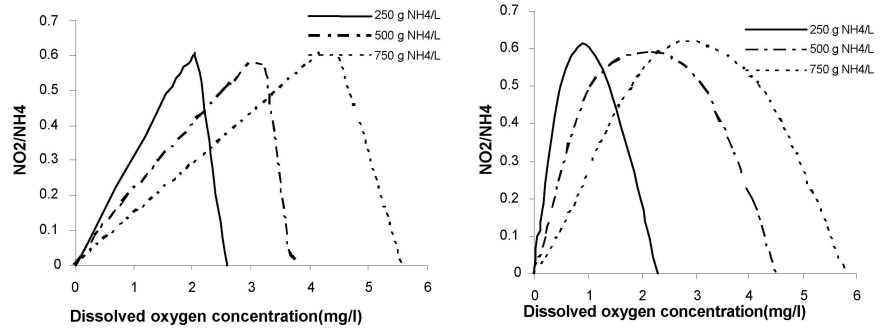

Fig. 5c: NH_4^+ concentration effect. Feeding flow rate of 0.8 L/h at 25°C

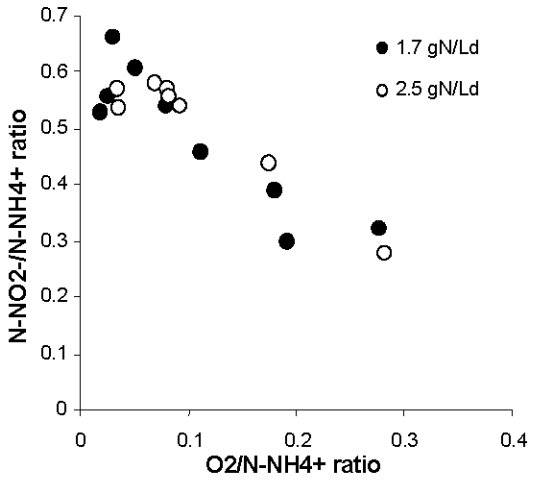

Fig. 6: Effect of O_2/N-NH_4^+ on the N-NO_2^- /N-NH_4^+ compounds distribution

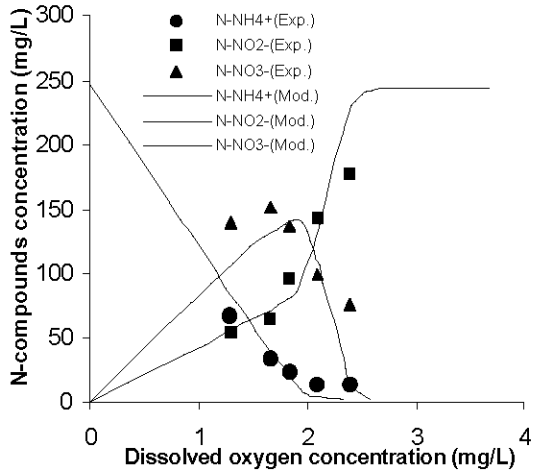

Fig. 7: Effect of DO concentration on N- compounds distribution

has two slopes; but at lower flow rate (0.2 L/h) the curve has just one slope, because at lower flow rates, the value of NO_2^- that has been produced is less and additionally the amount of NO_3^- is less too, so oxygen consumption rate is less and steady, but at higher flow rates, at first the oxygen curve will have more slope because of the NH_4^+ and NO_2^- consumption, when NH_4^+ is finished, the slope decreases because just NO_3^- is produced. In addition at higher feed flow rates NO_2^- concentration in the reactor increases and NO_3^- as well.

Effect of Ammonia Concentration: Figure 4, shows the effect of NH_4^+ concentration in feed. Three different concentrations have been used 250, 500 and 750 mg/L so that the first is in Figure (2-c).

We can see that with the increase of NH_4^+, the rate of consuming and producing of the material is smoother. In lower concentrations of NH_4^+ there are two cross points between NO_2^- and NO_3^-, one of which is at increasing of both of them and the other is when NO_2^- is consumed and NO_3 is produced because when NH_4^+ increases and O_2 is stable, O_2 isn't enough and in addition reactions are competing so NO_2^- is consumed but it has been substituted and NO_2^- consumption isn't clear but when NH_4^+ is less, O_2 is enough to consume all the NO_2^-. exactly that's why when NH_4^+ decreases, the difference between the slopes in every material is more clear, in addition the first cross point has done it sooner, as much as NH_4^+ increase, the cross point happens later.

Figure 5, shows the comparison between our simulation and the simulation in the reference for the experimental data. In all of them the vertical axis is NO2/NH4 ratio and the other is dissolved oxygen concentration. Figure.5.a is about temperature effect Figure 5.b feeding flow rate effect and Figure 5.c is NH_4^+ concentration effect. The results show desirable agreement between our simulation and the reference simulation but there is a little difference about the slope of charts its maybe because of some assumptions for example in the reference article liquid is imported from the top of the reactor and gas from the bottom but in our simulation both liquid and gas are imported from the bottom and this assumption effects the reaction time because it decreases the time that oxygen is taken to NH_4^+. When oxygen comes from the top, time increases so the oxygen consumption for a special ratio increases so the chart slop changes but the amount of oxygen for all of the NH_4^+ doesn't change.

In Figure 6, the experimental results of O2/N-NH_4^+ influences on the N-NO_2^- /N-NH_4^+ and in Figure 7 the effect of DO concentration on N- compounds distribution has been shown experimentally as well as the simulation, these figures are two samples, all the other figures (from reference [25] simulation) have been compared with the experimental once (in the original article) and have shown suitable agreement is indicated between them so we have compared our simulation results with the simulation of the reference article [25].

CONCLUSIONS

The effects of temperature, ammonium concentration and feed flow rate on nitrifying treatment of wastewater in an airlift reactor have been simulated in this article.

The simulation results showed that at higher temperatures, reactions are carried out quicker so the curve slope of $NH4^+$ and O2 consumption is higher. At higher feed flow rates at first the accumulation of $NO2^-$ increases, if there is enough O_2, the second reaction for producing $NO3^-$ will speed up until all amount of $NO2^-$ is consumed and we can see that with the increase of NH_4^+, the rate of consuming and producing of the material is smoother. All the simulation results were compared with experimental data that have shown a suitable agreement.

Nomenclature

C_d	Drag force coefficient
C_l	Lift force coefficient
C_μ	Constant in k-ε model
$C_{1\varepsilon}$	Model parameter in turbulent dissipation energy equation
$C_{2\varepsilon}$	model parameter in turbulent dissipation energy equation
d_B	[m] bubble diameter
F [N/m^2]	Interaction forces
Eo	Eotvos number

Greek symbols

σ_t	Prandtl number for turbulent energy dissipation rate
σ_k	Prandtl number for turbulent kinetic energy
τ_k [N/m^2]	Stress tensor of phase k
ε [m^2/s^3]	Turbulent dissipation rate per unit of mass
α_k	Volume fraction of phase k
μ_k [Pa.s]	Viscosity of phase k
ρ_k [kg/m^3]	Density of phase k
N [m^2/s]	Kinematic viscosity

Subscript

k	phase, k= G: gas phase, k=L: liquid phase

REFERENCES

1. Jianping, W., J. Xiaoqiang, P. Lei, W. Changlin and M. Guozhu, 2005. Nitrifying treatment of wastewater from fertilizer production in a multiple airlift loop bioreactor. Biochemical Engineering J., 25(1): 33-37.
2. Schmidt, I., O. Sliekers, M. Schmid, E. Bock, J. Fuerst, J.G. Kuenen S.M. Jetten and M. Strous, 2003. New concepts of microbial treatment processes for the nitrogen removal in wastewater. FEMS Microbiology Reviews, 27 (4): 481-492
3. Mosquera-Corral, A., F. Gonzalez, J.L. Campos and R. Mendez, 2005. Partial nitrification in a SHARON reactor in the presence of salts and organic carbon compounds. Process Biochemistry, 40 (9): 3109-3118.
4. Bernet, N., O. Sanchez, D. Cesbron, J.P. Steyer and J.P. Delgen`es, 2005. Modeling and control of nitrite accumulation in a nitrifying biofilm reactor, Biochemical Engineering J., 24(2): 173-183.
5. Jose´ L. Sanz and T. Ko¨chling, 2007, Molecular biology techniques used in wastewater treatment: An overview, Process Biochemistry, 42(2) 119-133.
6. Yamamoto, T., K. Takaki, T. Koyama and K. Furukawa, 2007. Novel Partial Nitritation Treatment for Anaerobic Digestion Liquor of Swine Wastewater Using Swim-Bed Technology. J. Bioscience Bioenging, 102(6): 497-503.
7. Shinohara, T., S. Qiao, T. Yamamoto, T. Nishiyama, T. Fujii, T. Kaiho, Z. Bhatti and Kenji Furukawa, 2009. Partial nitritation treatment of underground brine waste with high ammonium and salt content. J. Biosci. Bioeng, 108(4): 330-335.
8. Kuai, L. and W. Verstraete, 1998. Ammonium removal by the oxygen-limited autotrophic nitrification–denitrification system. Applied and Environmental Microbiol., 64(11): 4500-4506.
9. Schmidt, I., C. Hermelink, K. Van De Pas-Schoonen, M. Strous, H.J. Camp and J.G. Kuenen, 2002. Anaerobic ammonia oxidation in the presence of nitrogen oxides (NOX) by two different lithotrophs. Applied and Environmental Microbiol., 68(11): 5351-5357.
10. Fux, C., M. Boehler, P. Huber, I. Brunner and H. Siegrist, 2002. Biological treatment of ammonium-rich wastewater by partial nitritation and subsequent anaerobic ammonium oxidation (anammox) in a pilot plant. J. Biotechnol., 99(3) 295-306.
11. Choi, K.H., 2001. Hydrodynamic and mass transfer characteristics of external-loop airlift, reactors without an extension tube above the downcomer. Korean Chemical Engineering J., 18(2): 240-246.
12. Nikakhtari, H. and G.A. Hill, 2005. Hydrodynamic and oxygen mass transfer in an external Loop airlift bioreactor with a packed bed. Biochemical Engineering J., 27(2): 138-145.
13. Kouakou, E., T. Salmon, D. Toye, P. Marchot and M. Crine, 2005. Gas–liquid mass transfer in a circulating jet-loop nitrifying MBR. Chemical Engineering Sci., 60(22): 6346-6353.

14. Kim, D.J., D.I Lee and J. Keller, 2006. Effect of temperature and free ammonia on nitrification and nitrite accumulation in landfill leachate and analysis of its nitrifying bacterial community by FISH. Bioresource Technol., 97(3): 459-468.
15. Kim, D.J. and D. Seo, 2006. Selective enrichment and granulation of ammonia oxidizers in a sequencing batch airlift reactor. Process Biochemistry, 41(5): 1055-1062.
16. Kempen, R., J.W. Van and C.A. Mulder, 2001. Overview: full scale experience of the SHARON process for treatment of rejection water of digested sludge dewatering. Water Science and Technol., 44(1): 145-152.
17. Astrid, A. Van De Graaf, Peter De Bruijn, Lesley A. Robertson, S. Mikes, M. Jetten and Gijs Kuenen, 1996 Autotrophic growth of anaerobic ammonium-oxidizing micro-organisms in a fluidized bed reactor. Microbiology J., 142(8): 2187-2196.
18. Astrid A. Van de Graff, Arnold Muler Peter De Bruijn, S. Mike, M. Jetten, Lesley A. Robertson and J. Gijs Kueneni, 1995. Anaerobic Oxidation of Ammonium Is a Biologically Mediated Process. Applied and Environmental Microbiol., 61(4): 1246-1251.
19. Jetten, M., S.M. Strous, M. Van De Pas-Schoonen, K.T. Schalk, J. Van De Graaf and A.A. Logemann, 1998. The anaerobic oxidation of ammonium. FEMS Microbiol. Rev., 22(5): 421-37.
20. Dijkman, H. and M. Strous, 1999. Process for Ammonia Removal from Wastewater Water Research. Patent PCT/NL99/00446.
21. Teske, A., E. Alm, J.M. Regan, S. Toze, B.E. Rittmann and D.A. Stahl, 1994. Evolutionary Relationships among Ammonia- and Nitrite-Oxidizing Bacteria. J. Bacterol., 176(21): 6623-6630.
22. Versteeg, H. and W. Malalasekra, 1996. An introduction to computational fluid dynamics: The Finite Volume Method, 2nd Edition, pp: 96-102.
23. Tabib, M.V., S.A. Roy and J.B. Joshi, 2008. CFD simulation of bubble column-analysis of interface forces and turbulence models, Chemical Engineering J., 139(3): 589-614.
24. Sokolichin, A. and G. Eigenberger, 1999. Applicability of the standard turbulent model to the dynamic simulation of bubble columns: part I. Detailed numerical simulations, Chemical Engineering Sci., 54: 2273-2284.
25. Bernet, N., O. Sanchez, D. Cesbron, J.P. Steyer and J.P. Delgenes, 2005. Modeling and control of nitrite accumulation in a nitrifying biofilm reactor. Biochemical Engineering J., 24(2): 173-183.
26. Ruiz, G., D. Jeison, O. Rubilar, G. Ciudad and R. Chamy, 2006. Nitrification-denitrification via nitrite accumulation for nitrogen removal from wastewaters. Bioresource Technol., 97(2) 330-335.
27. Khin, T. and A.P. Annachhatre, 2004. Novel microbial nitrogen removal processes Biotechnology Advances, 22(7): 519-532.